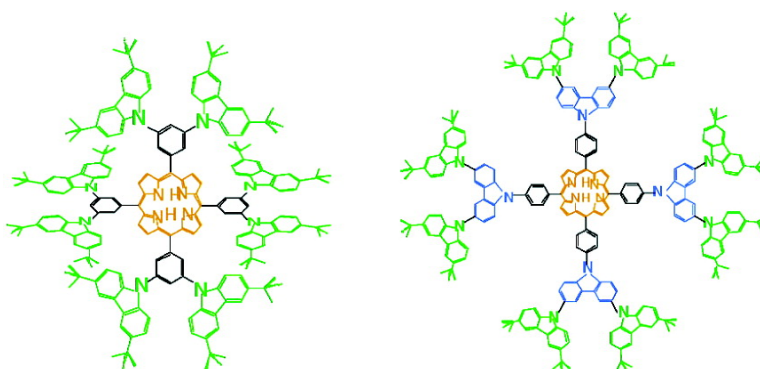


Dendrimers Made of Porphyrin Cores and Carbazole Chromophores as Peripheral Units. Absorption Spectra, Luminescence Properties, and Oxidation Behavior

Frdrique Loiseau, Sebastiano Campagna, Ahmed Hameurlaine, and Wim Dehaen

J. Am. Chem. Soc., 2005, 127 (32), 11352-11363 • DOI: 10.1021/ja0514444 • Publication Date (Web): 26 July 2005

Downloaded from <http://pubs.acs.org> on March 25, 2009



More About This Article

Additional resources and features associated with this article are available within the HTML version:

- Supporting Information
- Links to the 21 articles that cite this article, as of the time of this article download
- Access to high resolution figures
- Links to articles and content related to this article
- Copyright permission to reproduce figures and/or text from this article

[View the Full Text HTML](#)

Dendrimers Made of Porphyrin Cores and Carbazole Chromophores as Peripheral Units. Absorption Spectra, Luminescence Properties, and Oxidation Behavior

Frédérique Loiseau,[†] Sebastiano Campagna,^{*,†} Ahmed Hameurlaine,[‡] and Wim Dehaen^{*,‡}

Contribution from the Università di Messina, Dipartimento di Chimica Inorganica, Chimica Analitica e Chimica Fisica, via Sperone 31, I-98166, Messina, Italy, and University of Leuven, Department of Chemistry, Celestijnenlaan 200F, B-3001 Leuven, Belgium

Received March 7, 2005; E-mail: photochem@chem.unime.it; wim.dehaen@chem.kuleuven.ac.be

Abstract: Luminescent and redox-active porphyrin-based dendrimers of first and second generation have been synthesized, and their absorption spectra, photophysical properties, and oxidation behavior have been investigated, together with those of the corresponding aldehyde carbazole precursors. All the dendrimers contain a porphyrin core and carbazole-based chromophores as branches. The structural formulas of the new species are represented in Figures 1 and 2, with the corresponding schematizations. The absorption spectra of the aldehyde carbazole precursors **A1–A6** in dichloromethane exhibit intense transitions in the UV region, centered on the carbazole and benzaldehyde subunits. The lowest-energy absorption bands receive contribution from charge-transfer transitions. Compounds **A1–A6** are luminescent at room temperature in fluid solution; such a luminescence is attributed to twisted intramolecular charge-transfer excited states. The luminescence at 77 K in a rigid matrix is blue-shifted with respect to room-temperature emission and is assigned to locally excited states. Absorption spectra of the porphyrin-cored dendrimers **P1–P6** appear additive as they are constituted by visible bands due to porphyrin absorption and bands in the UV region due to transitions centered on the carbazole-based branches. Emission spectra of **P1–P6** both at 77 K and at room temperature are typical of porphyrin species and independent of excitation wavelength, indicating that the light collected by the peripheral chromophores is quantitatively transferred to the core. All the compounds exhibit a rich oxidation behavior in 1,2-dichloroethane solution, with reversible processes centered on the different carbazole subunits. Interaction between the different carbazole centers depends on the size of the spacer interposed.

Introduction

Dendrimers built from porphyrin subunits are quite interesting from many viewpoints: dendrimers containing porphyrins as cores and different branching units have been studied as synthetic analogues of biological systems, for example, to explore and clarify the redox properties of heme species,¹ as well as to investigate long-distance electron transfer at electrodes.² Dendrimers constructed from multiporphyrin units have been reported to play the role of light-harvesting antennae³ and, where properly connected with electron donor and acceptor groups, as charge-separation species for designing photochemical solar energy conversion devices operating at the molecular

level.⁴ Carbazole molecules are also quite interesting due to their own photophysical and redox properties: they exhibit relatively intense luminescence⁵ and undergo reversible oxidation pro-

[†] Università di Messina.

[‡] University of Leuven.

- (1) (a) Dandliker, P. J.; Diederich, F.; Gross, M.; Knobler, C. B.; Louati, A.; Sanford, E. M. *Angew. Chem., Int. Ed. Engl.* **1994**, *33*, 1739–1742. (b) Dandliker, P. J.; Diederich, F.; Zingg, A.; Gisselbrecht, J.-P.; Gross, M.; Louati, A. *Helv. Chim. Acta* **1997**, *80*, 1773–1801. (c) Weyermann, P.; Gisselbrecht, J.-P.; Boudon, C.; Diederich, F.; Gross, M. *Angew. Chem., Int. Ed.* **1999**, *38*, 3215–3219.
- (2) (a) Pollack, K. W.; Leon, J. W.; Fréchet, J. M. J.; Maskus, M.; Abruña, H. D. *Chem. Mater.* **1998**, *10*, 30–38. (b) Kimura, M.; Sugihara, Y.; Muto, T.; Hanabusa, K.; Shirai, H.; Kobayashi, N. *Chem.—Eur. J.* **1999**, *5*, 3495–3500. (c) Juris, A. In *Electron Transfer in Chemistry*; Balzani, V., Ed.; Wiley-VCH: Weinheim, 2001; Vol. 3, pp 655–714.

- (3) The literature on this topic is too vast to be exhaustively quoted. For some examples, see: (a) Collin, J.-P.; Harriman, A.; Heitz, V.; Odobel, F.; Sauvage, J.-P. *J. Am. Chem. Soc.* **1994**, *116*, 5679–5690. (b) Burrell, A. K.; Wasielewski, M. *J. Porphy. Phthalocya.* **2000**, *4*, 401–406. (c) Gust, D.; Moore, T. A.; Moore, A. L. *Acc. Chem. Res.* **2001**, *34*, 40–48. (d) Burrell, A. K.; Officer, D. L.; Plieger, P. G.; Reid, D. C. *W. Chem. Rev.* **2001**, *101*, 2751–2796. (e) Campagna, S.; Serroni, S.; Puntoriero, F.; Di Pietro, C.; Ricevuto, V. In *Electron Transfer in Chemistry*; Balzani, V., Ed.; Wiley-VCH: 2001; Vol. 5, pp 186–214. (f) Holten, D.; Bocian, D. F.; Lindsey, J. S. *Acc. Chem. Res.* **2002**, *35*, 57–69. (g) Guldi, D. M. *Chem. Soc. Rev.* **2002**, *31*, 22–37. (h) Seth, J.; Palaniappan, V.; Wagner, R. W.; Johnson, T. E.; Lindsey, J. S.; Bocian, D. F. *J. Am. Chem. Soc.* **1996**, *118*, 11194–11207. (i) Jiang, D.-L.; Aida, T. *J. Am. Chem. Soc.* **1998**, *120*, 10895–10901. (j) Nakano, A.; Yamazaki, T.; Nishimura, Y.; Yamazaki, I.; Osuka, A. *Chem.—Eur. J.* **2000**, *6*, 3254–3271. (k) Prodi, A.; Indelli, M. T.; Kleyerlaan, C. J.; Alessio, E.; Scandola, F. *Coord. Chem. Rev.* **2002**, *229*, 48–73. (l) Balzani, V.; Credi, A.; Venturi, M. *Molecular Devices and Machines. A Journey into the Nanoworld*; Wiley-VCH: Weinheim, 2003; Chapter 5.
- (4) (a) Kuciauskas, D.; Liddell, P. A.; Lin, S.; Johnson, T. E.; Weghorn, S. J.; Lindsey, J. S.; Moore, A. L.; Moore, T. A.; Gust, D. *J. Am. Chem. Soc.* **1999**, *121*, 8604–8614. (b) Nakano, A.; Osuka, A.; Yamazaki, T.; Nishimura, I.; Akimoto, S.; Yamazaki, I.; Itaya, A.; Murakami, M.; Miyasaka, H. *Chem.—Eur. J.* **2001**, *7*, 3134–3151. (c) Kodis, G.; Liddell, P. A.; de la Garza, L.; Clausen, P. C.; Lindsey, J. S.; Moore, A. L.; Moore, T. A.; Gust, D. *J. Phys. Chem. A* **2002**, *106*, 2036–2048. (d) Liddell, P. A.; Kodis, G.; de la Garza, L.; Moore, A. L.; Moore, T. A.; Gust, D. *J. Phys. Chem. B* **2004**, *108*, 10256–10265.

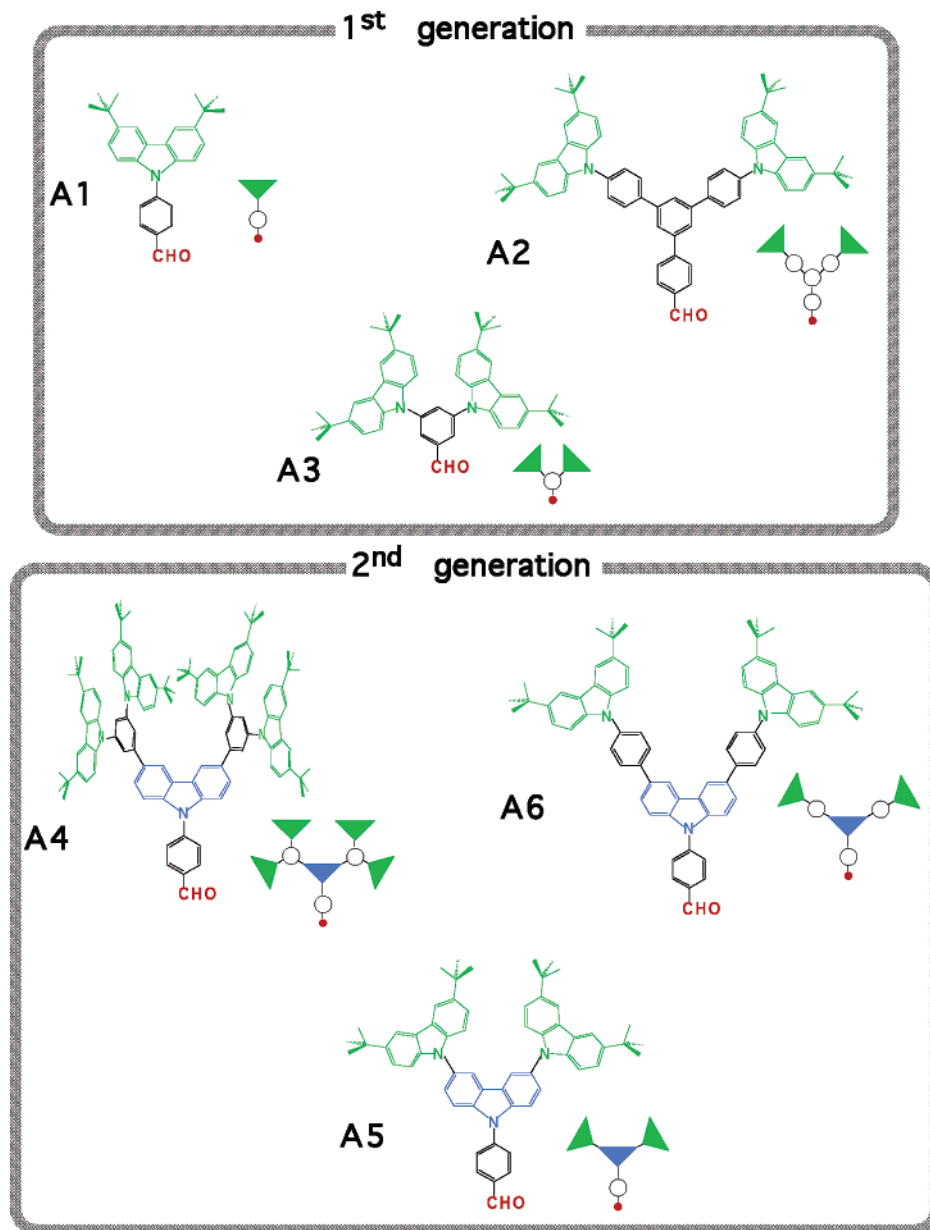


Figure 1. Structures of the aldehyde carbazole precursors of the first (A1–A3) and second generation (A4–A6) together with their schematic representations.

cesses which make them suitable as hole carriers.⁶ The properties of these carbazole systems prompted us to introduce first and second generation carbazole branches in dendrimers based on Ru(II) polypyridine complexes as cores.⁷ By taking advantage of the photophysical and redox properties of porphyrin and carbazole subunits, we have now synthesized new photo- and redox-active dendrimers of first and second generation incorporating porphyrin moieties as cores and various carbazole or multicarbazole groups as branches (or dendrons). Here we report the synthesis of these new species together with their absorption spectra, redox behavior, and luminescence properties. The same

properties of the carbazole precursors, in other words dendrons containing an aldehyde group, are also reported. The new species are shown in Figures 1 and 2, which also reports the abbreviations and symbols used to identify the compounds.

Results and Discussion

We recently described methods for the preparation of oligo-carbazole materials.⁸ The synthesis of the porphyrin-(oligo)-carbazole conjugates described here involves the preparation of aldehyde precursors by a multistep procedure via copper-catalyzed Ullmann coupling reactions or palladium-catalyzed Suzuki coupling reactions. Successive condensation with pyrrole is performed under Lindsey conditions:⁹ acid catalysis at high dilution followed by addition of oxidant.

(5) (a) Howell, A. G.; Taylor, A. G.; Phillips, D. *Chem. Phys. Lett.* **1992**, *188*, 119–125. (b) Yu, H.; Mohd Zain, S.; Eigenbrot, I. V.; Phillips, D. *Chem. Phys. Lett.* **1993**, *202*, 141–147. (c) Mohd Zain, S.; Hashim, R.; Taylor, A. G.; Phillips, D. *THEOCHEM* **1997**, *401*, 287–300.
 (6) Kido, J.; Hongawa, K.; Okuyama, K.; Nagai, K. *Appl. Phys. Lett.* **1993**, *63*, 2627–2629 and references therein.
 (7) McClenaghan, N. D.; Passalacqua, R.; Loiseau, F.; Campagna, S.; Verheyde, B.; Hameurlaine, A.; Dehaen, W. *J. Am. Chem. Soc.* **2003**, *125*, 5356–5365.

(8) (a) Hameurlaine, A.; Dehaen, W. *Tetrahedron Lett.* **2003**, *44*, 957–959. (b) Schaelaerckens, M.; Hendrickx, E.; Hameurlaine, A.; Dehaen, W.; Persoons, A. *Chem. Phys.* **2002**, *277*, 43–52.
 (9) Lindsey, J. S.; Schreyman, I. C.; Hsu, H. C.; Kearney, P. C.; Marguerettaz, A. M. *J. Org. Chem.* **1987**, *52*, 827–836.

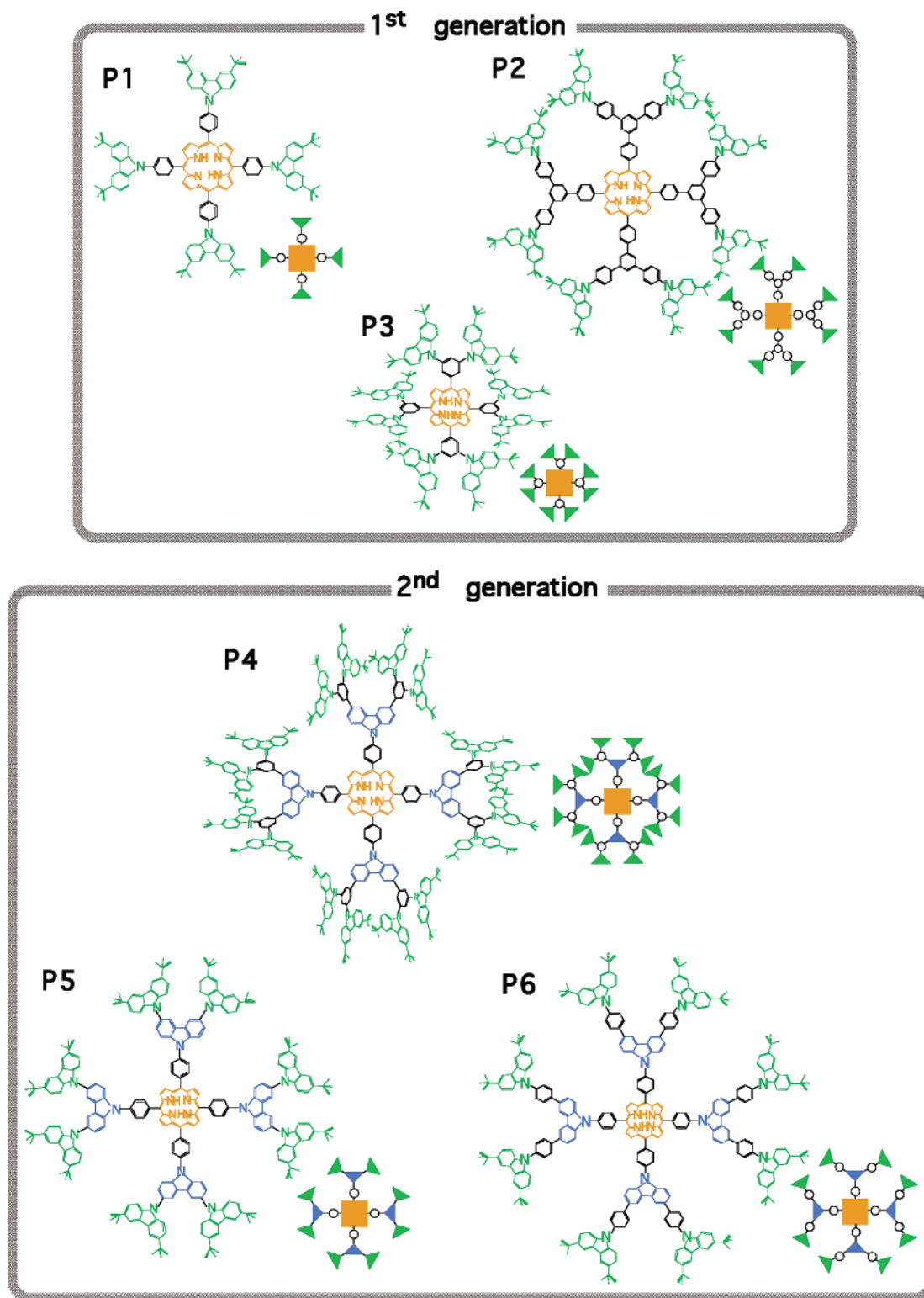


Figure 2. Structures of the porphyrin-cored dendrimers of the first (P1–P3) and second generations (P4–P6) together with their schematic representations.

The synthetic route to the aldehyde precursors involves a two- or three-step procedure starting from the corresponding mono-halogenated (iodo- or bromo-) carbazole species prepared following the described method⁸ converted into the functionalized aldehydes by lithiation in THF and quenching with DMF, with yields ranging from 25 to 75%. The aldehydes were converted into the corresponding tetrakis-*meso*-functionalized porphyrins in normal to good yields for this type of reaction

(15–30%). All the compounds were purified by column chromatography over silica gel. Further details are given in the Experimental Section.

Absorption Spectra. A. Aldehyde Carbazole Precursors.

The absorption spectra of the A1–A6 aldehyde precursors (Figure 3, Table 1) in dichloromethane exhibit intense transitions in the UV region. In particular, the broad band at about 230 nm, already present in 3,6-di(*tert*-butyl)carbazole,⁷ derives from

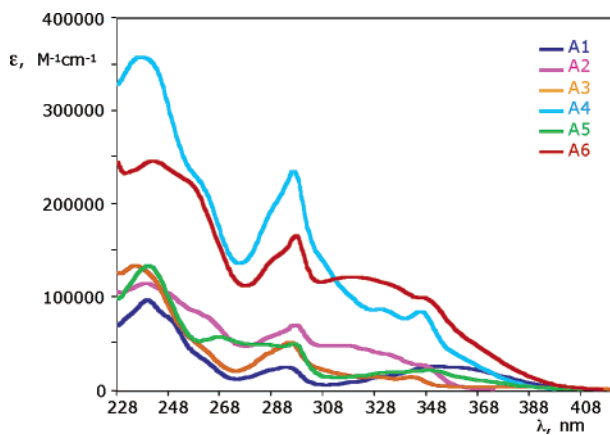


Figure 3. Absorption spectra of the aldehyde carbazole precursors **A1**–**A6** in dichloromethane solutions.

carbazole-centered transitions as well as the narrow band at about 295 nm, which is present in all the compounds. Interestingly, and in agreement with such an assignment, the molar absorbance of such bands parallels the number of carbazole moieties in **A1**–**A6**, with the larger values observed for **A4** (containing five carbazole subunits, although of two different types) and **A6** (three carbazole subunits) and the smaller value observed for **A1** (one carbazole subunit). Compound **A5** does not follow the rule, in that even though this compound contains three carbazole subunits, the molar absorbances of its 230 and 295 nm bands are significantly lower than expected (Table 1, Figure 3): this indicates that the carbazole moieties of this species strongly perturb one another, because of the direct connection between outer and inner carbazole moieties (where for *inner* carbazoles here we mean units directly connected to the phenyl-aldehyde group, where *outer* carbazoles are the units not directly connected to such a group, which can be seen also as *peripheral* ones). To the particular nature of the carbazole connections in **A5** is also linked the broad absorption in the 260–290-nm range (see Figure 3), which is absent in the other species.

As already reported for carbazole–phenanthroline compounds,⁷ charge-transfer (CT) transitions, in which the phenyl-aldehyde groups play the role of the acceptor and the carbazole subunits act as the electron donor, can also contribute to the absorption feature at wavelengths longer than 300 nm. Actually, the band between 300 and 400 nm which is present in **A1**–**A6** is solvent dependent, exhibiting a long tail in dichloromethane and THF (probably due to the CT contribution), which is lost in pentane, where the band also becomes structured (see Supporting Information). Detailed assignment of the various CT bands, anyway, is quite complicated, due to the different carbazoles involved.

B. Porphyrin-Cored Dendrimers. The absorption spectra of the porphyrin-cored **P1**–**P6** dendrimers in dichloromethane are shown in Figure 4, and the relevant data are gathered in Table 2. The absorption spectra of the dendrimers appear additive as they are made of visible bands which can be assigned to the porphyrin centers, namely, the intense Soret band at about 425 nm and the weaker Q-bands at longer wavelengths, and of bands which are mainly attributed to carbazole subunits in the UV region. Interaction of porphyrin and carbazoles seems negligible as far as the electronic absorption viewpoint is concerned. As expected, the absorption of the dendritic species

is much higher than the absorption of isolated porphyrin in the UV region, since strong carbazole-centered absorption bands, which rival the intense porphyrin Soret bands, are now present.

Oxidation Behavior. A. Aldehyde Carbazole Precursors. Oxidation behavior of aldehyde carbazoles has been investigated in 1,2-dichloroethane solution by means of differential pulse and cyclic voltammetries. Data are collected in Table 3, and two typical cyclic voltammograms are shown in parts a and b of Figure 5. In principle, each carbazole subunit of the compound can undergo a reversible one-electron oxidation at relatively mild potentials.^{6,7} This is in fact what has been observed, with the noticeable exception of **A5**. The oxidation potential of 3,6-di(*tert*-butyl)carbazole (+1.08 V vs standard calomel electrode (SCE)) is displaced to a more positive potential in **A1** (+1.30 V), as a consequence of the presence of the phenyl-aldehyde group which drains electron density from the carbazole center. The positive shift of the carbazole-based oxidation potential is slightly less pronounced for **A2**, probably due to the larger distance between the electron-withdrawing aldehyde groups and the carbazole units because of the presence of the additional phenyl rings. Interestingly, the oxidation process of this compound involves two electrons: the process is therefore assigned to simultaneous one-electron oxidation of each carbazole moiety, which are noninteracting one another as far as the redox behavior is concerned.¹⁰ Compound **A3** undergoes two one-electron reversible oxidation processes, separated by 120 mV. We assign such processes to successive oxidation of the two carbazole subunits. In contrast to the situation for **A2**, interaction between the carbazoles in **A3** is sizable and gives rise to oxidation splitting: this is attributed to the smaller “spacer” between the redox-active groups in **A3** (see structural formulas in Figure 1). Compound **A4** is the species exhibiting the richest oxidation behavior within the **A1**–**A6** series: indeed the voltammograms of this species indicate that **A4** undergoes two successive bielectronic processes, followed by a third oxidation process involving one electron. The first process is assigned to simultaneous, one-electron oxidation of two noninteracting outer carbazole subunits linked to different phenyls, the second oxidation process is attributed to simultaneous, one-electron oxidation of the other two outer carbazoles, and the third process is assigned to the inner carbazole. Separation between first and second oxidation processes is related to the interaction between two carbazole subunits linked to the same phenyl, and is 130 mV, in full agreement with the separation between the first and second processes of **A3** (see above) assigned to the same effect.

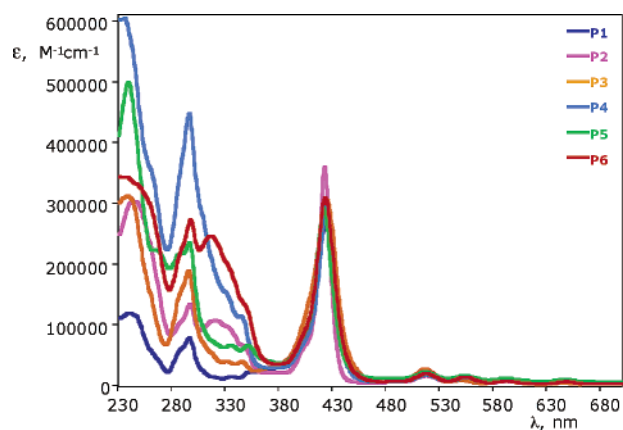
Compound **A5** exhibits two successive one-electron oxidation processes. This compound is somewhat different from the others in that the carbazole subunits are directly connected to one another, without the presence of interposed phenyl rings. In fact, this compound is the only one in the series for which the number of reversible oxidation processes is less than the number of carbazole moieties. The two processes here are attributed to successive one-electron oxidations of the outer carbazoles. The presence of the directly connected inner carbazole contributes to keep the oxidation processes at less positive potentials than

(10) For a thorough discussion of the redox behavior of noninteracting centers, see: Flanagan, J. B.; Margel, S.; Bard, A. J.; Anson, F. C. *J. Am. Chem. Soc.* **1978**, *100*, 4248–4253. For recent applications, see: Venturi, M.; Serroni, S.; Juris, A.; Campagna, S.; Balzani, V. *Top. Curr. Chem.* **1998**, *197*, 193–202, and refs. therein.

Table 1. Spectroscopic and Photophysical Data of the Aldehyde Carbazole Precursors **A1–A6** in Deaerated Dichloromethane Solution (298 K) or in butyronitrile Rigid Matrix (77 K)

Compound	Absorption λ_{\max} , nm (ϵ , $M^{-1}cm^{-1}$)	Luminescence 298 K		Luminescence 77 K	
		λ_{\max} , nm	τ , ns	λ_{\max} , nm	τ , ns
CZ ^a 	235 (46000) 293 (23100) 325 (3500)	352	8.4	352	16.1
PhCZ ^b 	242 (48700) 293 (28400) 343 (12200)	357	5.5	356	11.4
A1 	240 (96700) 294 (24200) 350 (24600)	510	3.1	424	5.1
A2 	240 (114500) 298 (69500) 314 (47700)	535	14.5	422	12.6
A3 	236 (133200) 296 (50400) 342 (13300)	529	4.6	487	2.9; 12.6
A4 	238 (358000) 296 (235200) 346 (84200)	486	7.0	412	3.2; 8.4
A5 	240 (133100) 268 (56200) 296 (49300) 348 (20800)	555	5.6	452	8.5
A6 	242 (246200) 298 (164700) 320 (121300)	522	5.9	432	3.8

^a CZ is for 3,6-di(*tert*-butyl)carbazole. ^b PhCZ is for (*N*-phenyl)3,6-di(*tert*-butyl)carbazole.

**Figure 4.** Absorption spectra of the porphyrin-cored dendrimers **P1–P6** in dichloromethane solutions.

the other species. The inner carbazole is not oxidized within the potential window (or, better to say, before irreversible oxidation takes place, see later) because it is strongly connected

with two oxidized carbazoles so its highest-occupied molecular orbital (HOMO) is strongly stabilized.

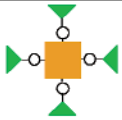
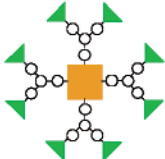
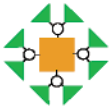
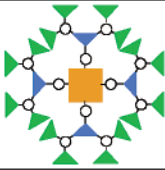
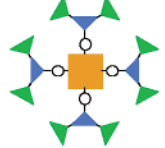
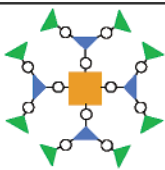
Finally, compound **A6** exhibits a first process, bielectronic in nature, followed by a mono-electronic process. The first process is assigned to simultaneous oxidation of the two outer, noninteracting carbazole units (in this case the “spacer” is roughly identical to the one contained in **A4**, which “separates” the redox-active units by the electrochemical viewpoint), and the second one is attributed to the inner carbazole group.

All the compounds exhibit an irreversible oxidation process at about +1.65 V, which has not been investigated. This process, anyway, is probably due to the well-known electropolymerization of carbazole derivatives,¹¹ as suggested by one of the reviewers.

B. Porphyrin-Cored Dendrimers. The porphyrin-cored dendrimers **P1–P6** contain a large number of redox-active subunits, including all the carbazole centers and the porphyrin

(11) Mengoli, G.; Musiani, M. M.; Schreck, B.; Zecchin, S. *J. Electroanal. Chem.* **1988**, 73–86.

Table 2. Spectroscopic and Photophysical Data of the Porphyrin-Cored Dendrimers **P1–P6** in Deaerated Dichloromethane Solution (298 K) or in butyronitrile Rigid Matrix (77 K)

Compound	Absorption λ_{\max} , nm (ϵ , $M^{-1}cm^{-1}$)	Luminescence 298 K			Luminescence 77 K	
		λ_{\max} , nm	τ , ns	Φ	λ_{\max} , nm	τ , ns
TPP^a 	299 (25900) 370 (25800) 416 (280200)	650	10.3	0.036	644	16.3
P1 	240 (117400) 293 (75900) 348 (20200) 424 (266100)	655	9.2	0.047	650	13.7
P2 	247 (299700) 295 (127500) 320 (102300) 422 (357600)	654	9.8	0.051	651	12.4
P3 	239 (308800) 295 (186400) 345 (37600) 424 (302300)	649	9.7	0.030	643	17.2
P4 	237 (599800) 296 (449500) 345 (119800) 424 (294500)	655	9.8	0.047	644	9.8
P5 	240 (499000) 266 (210600) 293 (218900) 351 (60800) 422 (280300)	654	9.6	0.048	647	14.1
P6 	239 (339000) 295 (268700) 316 (242000) 423 (304700)	655	9.7	0.047	658	13.9

^a TPP is for *meso*-tetraphenylporphyrin.

core itself. For example, in principle up to 21 redox-active groups are present in **P4**: 16 outer carbazoles, 4 inner carbazoles, and 1 porphyrin subunit (here, for *inner* carbazoles we mean those directly connected with the porphyrin phenyl rings and for *outer* carbazoles we mean the peripheral ones). So the oxidation behavior of these systems is expected to be very rich (see Table 3). Actually, **P1** undergoes a single reversible oxidation process at +1.28 V, which involves four electrons. Compound **P1** is derived from **A1**, and indeed the oxidation potential of the process is quite close to that exhibited by its parent aldehyde precursor (+1.30 V), so the oxidation of **P1** can be straightforwardly assigned to simultaneous one-electron oxidation of the four noninteracting carbazole units. The situation is similar for **P2**, which is derived from **A2**: **P2** indeed undergoes one oxidation process at +1.20 V (compare

with the oxidation potential of **A2**, +1.21 V), which involves eight electrons; the process is therefore assigned to simultaneous one-electron oxidation of the eight carbazole subunits. Carbazole subunits belonging to the same “dendron” are oxidized simultaneously since their spacer is large enough to separate them electrochemically, as is the case for **A2**. **P2** also undergoes an irreversible process at about +1.37 V, which is attributed to porphyrin oxidation. Quite surprisingly, **P2** is the only compound of the series in which porphyrin oxidation is evidenced (see Table 3). A possible explanation could be linked to the presence in **P2** of a larger aromatic spacer (the four phenyl system, see Figure 2) interposed between the redox-active carbazole groups and the porphyrin core. Such a larger spacer can better isolate branching and core sites, allowing the occurring of the porphyrin oxidation at mild potentials.¹²

Table 3. Oxidation Potentials of the Compounds in Argon-Purged 1,2-Dichloroethane Solution^a

Compound	$E_{1/2\text{ox}}$, V vs SCE
A1 	+1.30 [1]; +1.64*
A2 	+1.21 [2]; +1.63*
A3 	+1.31 [1]; +1.43 [1]; +1.66*
A4 	+1.24 [2]; +1.37 [2]; +1.59 [1]
A5 	+1.08 [1]; +1.22 [1]; +1.64*
A6 	+1.16 [2]; +1.44 [1]; +1.65*
P1 	+1.28 [4]; +1.67*
P2 	+1.20 [8]; +1.37*
P3 	+1.28 [4]; +1.40 [4]; +1.66*
P4 	+1.23 [8]; +1.41 [8]; +1.65*
P5 	+1.05 [4]; +1.21 [4]; +1.65*
P6 	+1.09*; +1.43*

^a Number of exchanged electrons is given in brackets. ^b Irreversible processes.

The splitting of the two carbazole oxidations showed by **A3**, for which there is a sizable carbazole–carbazole interaction (see above) is reflected in the oxidation behavior of **P3**. Such a compound actually exhibits two reversible processes, each one involving four electrons; the oxidations are here attributed to two series of one-electron oxidations involving a carbazole

(12) Interaction between the oxidized carbazole branches and the porphyrin core (in the **P1**–**P6** compounds, the carbazoles, or at least some of them, are the first to be oxidized, so the interaction involves porphyrin core and oxidized branches) is expected to move porphyrin-centered oxidation to more positive potentials. Such an interaction is depending on the spacer between core and branching subunits.

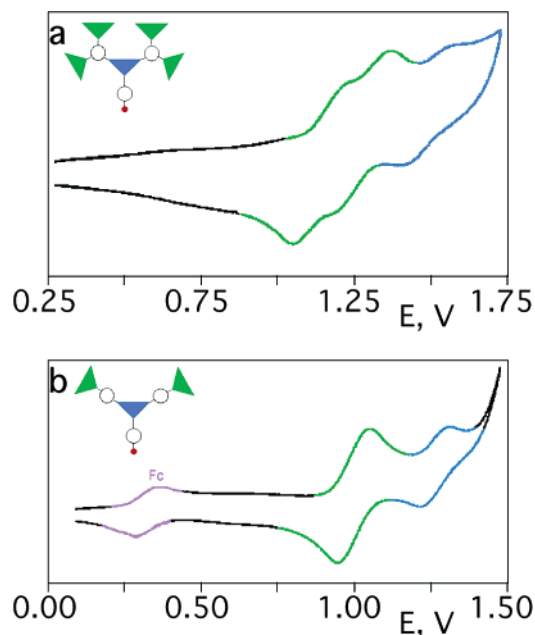


Figure 5. Cyclic voltammograms of **A4** (a, scan rate = 200 mV/s) and **A6** (b, scan rate, 50 mV/s) in argon-purged 1,2-dichloroethane solutions.

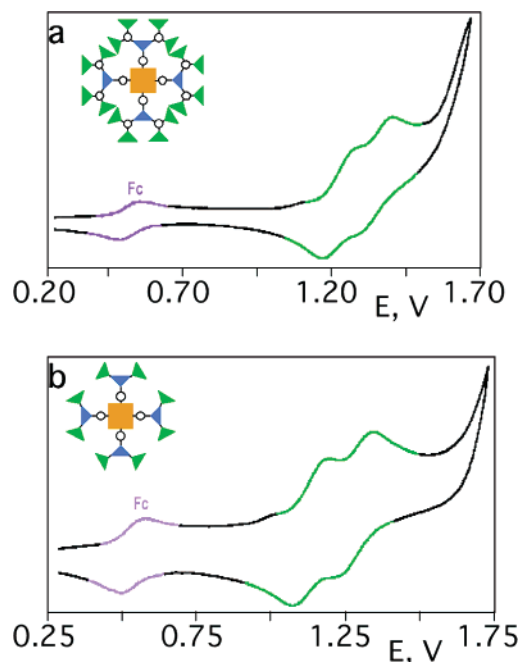


Figure 6. Cyclic voltammograms of **P4** (a, scan rate = 20 mV/s) and **P5** (b, scan rate = 50 mV/s) in argon-purged 1,2-dichloroethane solutions.

belonging to different branching units. The separation of the oxidation processes is 120 mV (Table 3), in agreement with the splitting of the oxidation processes of the parent **A3** species.

Compound **P4** undergoes two successive eight-electrons processes, separated by 180 mV (Table 3, Figure 6a). The first oxidation is assigned to simultaneous one-electron oxidation processes involving eight outer carbazole subunits, each of them linked to different outer phenyls, and the second oxidation process is attributed to simultaneous one-electron oxidation of the other, not yet oxidized, eight outer carbazole subunits. The inner carbazoles are not oxidized at a potential less negative than 1.66 V, at which an irreversible process takes place that obscures any other process.

The absence of the inner carbazole oxidation, surprising as it was for **P4**, is expected for **P5**, since inner carbazole oxidation is not observed in **A5** (see above). Compound **P5** undergoes two four-electron oxidation processes (see Figure 6b), assigned to sequential processes involving simultaneous one-electron oxidation of the outer carbazoles, following the scheme operating in **P3** and **P4**, while inner carbazole oxidation is indeed not observed.

Compound **P6** exhibits an ill-behaved oxidation, in that it undergoes two irreversible processes at mild potentials (Table 3). The reason of this behavior, which represents an exception within the series, has not been investigated.

Luminescence Properties. A. Aldehyde Carbazole Precursors. The carbazole-containing aldehyde species here investigated are compounds in which strong electron-donor groups (the carbazole moieties) are interfaced with a good electron-acceptor moiety (the benzaldehyde). As such, CT transitions and excited states at relatively low energies are expected, as evidenced by the absorption spectra (see above). Moreover, the similitude of **A1–A6** with 4-dimethylaminobenzonitrile and similar compounds, which can give rise to twisted intramolecular charge-transfer (TICT) excited state and luminescence,¹³ is evident. TICT excited states are quite common in species containing donor and acceptor subunits and in which rotation of part of the molecule with respect to the other is allowed. We start the discussion by assuming that TICT states are involved in the luminescence properties of the present systems. To briefly summarize, within this assumption upon light excitation in the CT bands an electron from the donor carbazole-centered orbital is initially transferred to a benzaldehyde-centered orbital, with formation of an excited state with partial CT character, although delocalized over all the molecule. This state maintains the conformation of the ground state (having roughly coplanar HOMOs and lowest-unoccupied molecular orbital (LUMO)s) and can be called locally excited (LE), analogously to *N,N*-dimethylaminobenzonitrile and similar compounds.^{13,14} Within the lifetime of the LE excited state and depending on several factors including solvent effects, HOMO and LUMO orbitals can be decoupled by internal (intramolecular) rotation of the donor part of the molecule compared to the acceptor part. In this way, a *net* charge separation is obtained and the relaxed excited state is termed TICT. TICT emission can then take place, at energies lower than the LE emission, and usually also with a broad spectral shape.^{13,14} In the **A1–A6** compounds here studied, TICT emission at room temperature in fluid solution is supported by the following results: (i) the large energy difference between lower-energy absorption bands and emission bands (Table 1), which rules out a singlet $\pi-\pi^*$ emission; (ii) the broad shape of the emission spectra (Figure 7); the lifetimes of the emission, which rule out a triplet assignment (Table 1). The large polar character of the emitting excited state, in good agreement with a TICT assignment, is also supported by the

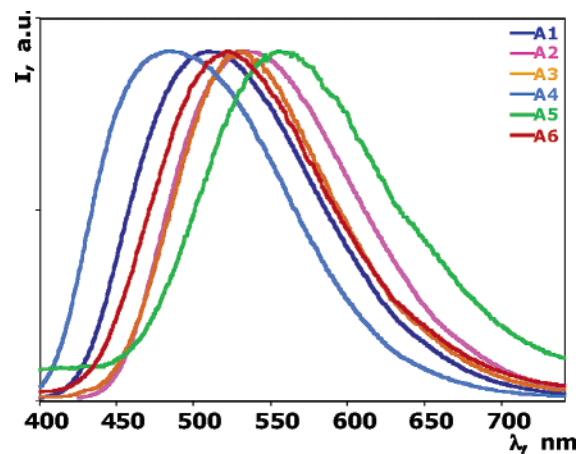


Figure 7. Room-temperature uncorrected emission spectra of the aldehyde carbazole precursors **A1–A6** in dichloromethane solutions. Corrected values of the emission maxima are given in Table 1.

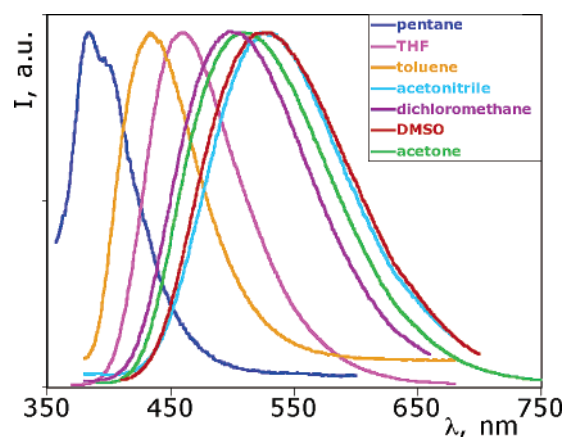


Figure 8. Room-temperature emission spectra of **A1** in solvents of different polarities.

solvent dependence of the emission, as shown in Figure 8 for compound **A1**. For such a species, as well as for all the other species (not shown), the emission band strongly moves to the blue on decreasing the polar nature of the solvent, reaching a maximum at 388 nm in pentane: in this solvent the emission spectrum also becomes structured, similar to the carbazole-centered emission.⁷ We suggest that the excited state responsible for the emission in pentane is the LE state, with the TICT state highly destabilized in such a solvent. A further indication for a large conformational movement (as in TICT formation) on the excited-state surface prior to emission comes from plotting the emission maximum energy as a function of the Lippert solvent polarity.¹⁵ In this type of “Lippert–Mataga” plots,¹⁶ the slope is a measure of the variation in dipole moment upon excitation and a break in the linear relationship suggests the presence of two different excited states. Indeed, the emission maximum energy in pentane deviates from the linear relationship followed by the emission energy in the other solvents.^{17,18}

To discuss in detail the differences in emission energy within the series of compounds (Table 1) is not an easy task: the donor orbital is not necessarily localized on the subunits corresponding

(13) (a) Grabowski, Z. R.; Rotkiewicz, K.; Siemiarczuk, A.; Cowley, D. J.; Baumann, W. *Nouv. J. Chim.* **1979**, *3*, 443–447. (b) Grabowski, Z. R.; Dobkowski, J. *Pure Appl. Chem.* **1983**, *55*, 245–247. (c) Bonacic-Koutecky, V.; Michl, J. *J. Am. Chem. Soc.* **1985**, *107*, 1765–1766. (d) Rettig, W. *Angew. Chem., Int. Ed. Engl.* **1986**, *25*, 971–988. (e) Lippert, E.; Rettig, W.; Bonacic-Koutecky, V.; Heisel, F.; Miehé, J. A. *Adv. Chem. Phys.* **1987**, *68*, 1–13. (f) (e) Klessinger, M.; Michl, M. *Excited States and Photochemistry of Organic Molecules*; VCH: New York, 1995.

(14) (a) Rettig, W.; Lippert, E. *J. Mol. Struct.* **1980**, *61*, 17–24. (b) Rettig, W.; Gleiter, R. *J. Phys. Chem.* **1985**, *89*, 4676–4680. (c) Rettig, W. In *Supramolecular Photochemistry*; Balzani, V., Ed.; Reidel: Dordrecht, The Netherlands, 1987; p 329 and references therein.

(15) Reichardt, C. *Chem. Rev.* **1994**, *94*, 2319–2358.

(16) Mataga, N.; Kubota, T. *Molecular Interactions and Electronic Spectra*; Dekker: New York, 1970.

(17) We would like to thank one of the reviewer for suggesting us to use the “Lippert–Mataga” plots.

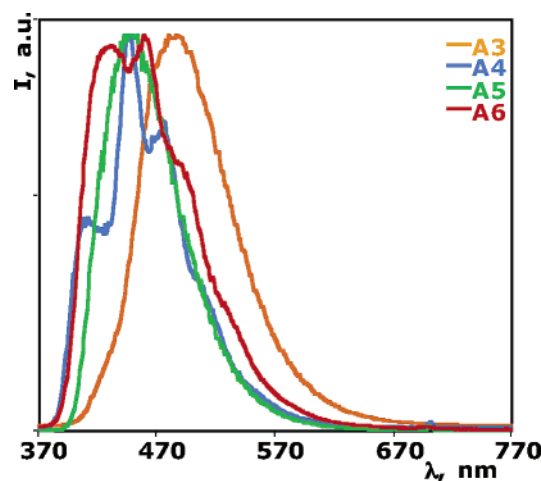


Figure 9. Uncorrected emission spectra of the aldehyde carbazole precursors **A3**–**A6** in butyronitrile rigid matrix at 77 K (emission spectra of **A1** and **A2** are not shown, in that they are very similar to the one of **A4**). Corrected values of the emission maxima are given in Table 1.

to the first oxidation process, since inner carbazoles, when inner and outer subunits are present, are expected to be more strongly involved in the spectroscopic and photophysical processes for Coulombic reasons (larger separation between positive and negative charges in TICT states, as the case when outer carbazole are involved, would lead to destabilization), so correlation between redox and spectroscopic data is less useful. Different carbazole positions with respect to the benzaldehyde group (i.e., meta or para substitution) also add complications. Most likely this topic would require a theoretical approach, which is out of the aims of this work.

Compounds **A1**–**A6** also exhibit luminescence at 77 K (Table 1, Figure 9), which is strongly blue-shifted with respect to room-temperature emission in all cases except **A3**. Moreover, the spectra become structured and look like the mirror image of the lowest-energy absorption band. We assign the 77 K emission of all the compounds but **A3** to the LE excited states. The internal twist necessary to form the TICT state is indeed inhibited in a rigid glass, so emission can happen from the initially prepared LE states. **A3**, as mentioned above, is the exception, as the blue-shift of the emission on passing to low temperature in a rigid matrix is much smaller than for the other species and the 77 K spectrum does not exhibit a structure. It should be noted that this species is particularly crowded around the phenyl ring, so the carbazole subunits cannot be coplanar with the phenyl. In other words, the ground state should have a structure quite similar to the one typical for the TICT state, so that TICT-type emission is also probable at 77 K. However, a contribution from the LE emission, as suggested by the double exponential decay, cannot be excluded.

B. Porphyrin-Cored Dendrimers. All the compounds **P1**–**P6** exhibit relatively intense emission, both at 77 K in a rigid

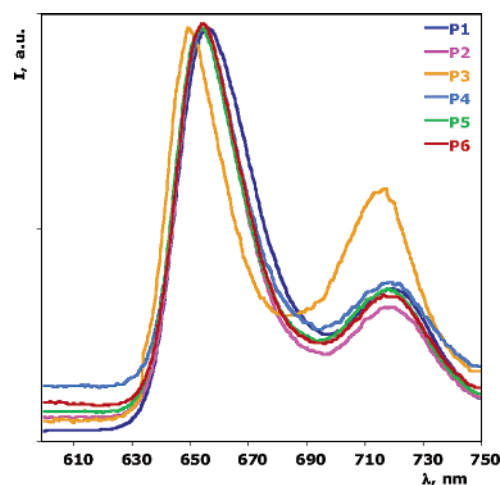


Figure 10. Room-temperature uncorrected emission spectra of the porphyrin-cored dendrimers **P1**–**P6** in dichloromethane solutions. Corrected values of the emission maxima are given in Table 2.

matrix and at room temperature in a fluid solution (Table 2, Figure 10). The spectra are typical of porphyrin emission,¹⁹ so they are assigned in all the cases to the porphyrin core subunits. Interestingly, the emission spectra are independent of excitation wavelength (within the range 320–630 nm) and excitation spectra fairly overlap the absorption spectra. This indicates that the light collected by the peripheral carbazole chromophores is transferred quantitatively to the porphyrin core. Therefore, **P1**–**P6** are efficient light-harvesting antennae, with the porphyrins acting as the energy trap.

Compound **P3** warrants additional comments, since its luminescence quantum yield is significantly lower and its emission spectrum exhibits a different ratio between first and second vibrational maxima than the other species (Table 2, Figure 10). An increased intensity of the second vibrational band compared to the first one could suggest a larger difference between ground state and emitting state nuclear coordinates. This also would take into account for the reduced quantum yield, since large distortion of the emitting state translates into more favorable Franck–Condon factors for nonradiative decay processes. However, this should be reflected in a shorter lifetime, and this is not the case. So, reasons for the slightly anomalous photophysical properties of **P3** should possibly lie in the radiative rate constant of the emitting state. Indeed, smaller molar absorbance of the low-energy bands in the absorption spectrum of **P3** compared to the other species of the series (namely, the 645- and 550-nm features) can be noted, which points out to a smaller oscillator strength for the radiative transitions between the ground and the emitting state in **P3**. Steric crowding around the phenyl rings bearing the carbazole substituents, as already mentioned for **A3**, could be responsible for this behavior, leading to a somewhat distorted porphyrin plane.

Conclusions

Six novel dendrimers constituted by a porphyrin core and four repetitive carbazole-based branching subunits have been

(18) In principle, most of the experimental results that lead to a TICT assignment for the room-temperature emission of **A1**–**A6** could also support a twisted ground state that becomes more planar upon CT excitation. However such an alternative interpretation can hardly justify the complete charge-transfer calculated from the Lippert–Mataga plot (in fact, assuming a charge separation over a distance of 3 Å in the excited emitting state and a variation in the dipole moment between ground and emitting states of ca. 12 D (from the slope of the Lippert plot), about 1 electron is calculated to be involved in the CT process, i.e., complete charge transfer) and, even more important, cannot explain the 77 K luminescence properties of **A3** (see later in the main text).

(19) (a) Kalyanasundaram, K. *Photochemistry of Polypyridine and Porphyrin Complexes*; Academic Press: London, 1991. (b) Gust, D.; Moore, T. A. In *The Porphyrin Handbook, Volume 8, Electron Transfer*; Kadish, K. M., Smith, K. M., Guillard, R., Eds.; Academic Press: San Diego, 2000; p 153 and references therein.

prepared, along with their corresponding benzaldehyde carbazole precursors. The absorption spectra, luminescence properties at room temperature in fluid solution and at 77 K in rigid matrix, and oxidation behavior of all the compounds have been investigated. Absorption spectra of the dendrimers are additive, covering both UV and visible regions of the spectrum. Oxidation behavior of the compounds is quite rich, with reversible processes mostly centered on the carbazole moieties. Differences in electronic communication between the subunits have been highlighted according to the structure of the dendrons. All the aldehyde carbazole precursors are luminescent at room temperature and at 77 K. In fluid solution, their emission is attributed to TICT excited states, whereas in rigid matrix, where internal twist is inhibited, emission is assigned to locally excited states. With concern for the porphyrin-cored dendrimers, the luminescence both at room temperature and at 77 K is typical of the porphyrin moieties, whatever the excitation wavelength is. Moreover, excitation spectra fairly overlap the absorption spectra, showing that all the light absorbed by the peripheral carbazole chromophores is transferred to the porphyrin core. The new dendrimers can therefore be regarded as efficient light-harvesting antenna systems, with the porphyrin subunits acting as the energy trap.

Experimental Section

Materials and Methods. NMR spectra were acquired on commercial instruments (Bruker Avance 300 MHz or Bruker AMX 400 MHz), and chemical shifts (δ) are reported in parts per million referenced to internal residual solvent protons (^1H) or the carbon signal of deuterated solvents (^{13}C). Mass spectrometry data were obtained with an HP MS apparatus 5989A (chemical ionization (CI), CH_4) or a Micromass Quattro II apparatus (electrospray ionization (ESI), solvent mixture: $\text{CH}_2\text{Cl}_2/\text{MeOH} + \text{NH}_4\text{OAc}$). Melting points were recorded on a Reichert Thermovar instrument; values are uncorrected.

Electronic absorption spectra were recorded on a Jasco V-560 spectrophotometer. For steady-state luminescence measurements, a Jobin Yvon-Spex Fluoromax 2 spectrofluorimeter was used, equipped with a Hamamatsu R3896 photomultiplier, and the spectra were corrected for photomultiplier response using a program purchased with the fluorimeter. For the luminescence lifetimes, an Edinburgh OB 900 time-correlated single-photon-counting spectrometer was used in the nanosecond range. As excitation sources, a Hamamatsu PLP 2 laser diode (59-ps pulse width at 408 nm) and the nitrogen discharge (pulse width = 2 ns at 337 nm) were employed. Luminescence quantum yields have been calculated by the optically diluted method.²⁰

Electrochemical measurements were carried out in argon-purged 1,2-dichloroethane at room temperature with a PAR 273 multipurpose equipment interfaced to a PC. The working electrode was a glassy carbon (8 mm², Amel) electrode. The counterelectrode was a Pt wire, and the reference electrode was an SCE separated with a fine glass frit. The concentration of the complexes was about 5×10^{-4} M. Tetrabutylammonium hexafluorophosphate was used as supporting electrolyte, and its concentration was 0.05 M. Cyclic voltammograms were obtained at scan rates of 20, 50, 200, and 500 mV/s. For reversible processes, half-wave potentials (vs SCE) were calculated as the average of the cathodic and anodic peaks. The criteria for reversibility were the separation of 60 mV between cathodic and anodic peaks, the close-to-unity ratio of the intensities of the cathodic and anodic currents, and the constancy of the peak potential on changing scan rate. The number of exchanged electrons was measured with differential pulse voltammetry (DPV) experiments performed with a scan rate of

20 mV/s, a pulse height of 75 mV, and a duration of 40 ms and by taking advantage of the presence of ferrocene used as the internal reference.

Experimental uncertainties were as follows: absorption maxima, ± 2 nm; molar absorption coefficients, 10%; emission maxima, ± 5 nm; excited-state lifetimes, 10%; luminescence quantum yields, 20%; redox potentials, ± 10 mV.

Synthesis. General Notes. All manipulations were performed under a dry nitrogen atmosphere using standard techniques. THF was distilled over sodium/benzophenone immediately before use. 3,6-Di(*tert*-butyl)-carbazole²¹ was prepared according to literature procedures.

4-[3,6-Bis(*tert*-butyl)carbazol-9-yl]benzaldehyde (A1). Under a dry atmosphere of nitrogen, a solution of *n*-BuLi in hexane 2.5 M (0.4 g, 6.2 mmol) was added dropwise to 3,6-bis(*tert*-butyl)-9-(4-iodophenyl)-carbazole (2 g, 4.15 mmol) in anhydrous THF (10 mL) cooled at -78 °C, and the mixture was allowed to stir for 15 min. Then, anhydrous DMF (0.6 g, 8.3 mmol) was added, and the mixture was vigorously stirred for additional 15 min. The cooling bath was removed, and the temperature was allowed to rise to room temperature. After the mixture was stirred for 2 h at room temperature, water was added. After extraction with dichloromethane, the organic layer was dried over anhydrous magnesium sulfate and the solvent was removed under reduced pressure. The residue was purified by column chromatography over silica gel with a mixture of hexane/dichloromethane (7:3) as eluent to give 0.85 g of **A1** as a yellow solid in 55% yield. mp 154–156 °C. ^1H NMR (300 MHz, CDCl_3 , ppm): δ 10.1 (s, 1 H, CHO), 8.13 (d, $^4J = 1.8$ Hz, 2H), 8.10 (d, $^3J = 8.4$ Hz, 2 H), 7.78 (d, $^3J = 8.4$ Hz, 2H), 7.46 (m, 4H), 1.48 (s, 18H). ^{13}C NMR (75 MHz, CDCl_3 , ppm): δ 191.4, 144.3, 138.8, 134.6, 131.8, 126.6, 124.5, 124.3, 116.9, 109.7, 35.2, 32.4. MS (CI) *m/z*: 384 (MH^+), 368 ($\text{M}^+ - \text{CH}_3$), 328 ($\text{M}^+ - \text{t-Bu}$).

3,5-Bis[3,6-bis(*tert*-butyl)carbazol-9-yl]phenyl]biphenyl-4-carbaldehyde (A2). The synthesis was performed according to the synthetic procedure described for **A1** using 1-(*p*-bromophenyl)-3,5-bis[*p*-[3,6-bis(*tert*-butyl)carbazol-9-yl]phenyl]benzene (0.47 g, 0.5 mmol), *n*-BuLi (0.05 g, 0.75 mmol), and DMF (0.07 g, 1 mmol) in THF (10 mL). This gave, after purification by column chromatography over silica gel with a mixture of heptane/chloroform (8:2 to 5:5) as eluent, 0.1 g of **A2** as a white solid in 23% yield. mp > 300 °C. ^1H NMR (400 MHz, CDCl_3 , ppm): δ 10.11 (s, 1 H, CHO), 8.16 (s, 4 H), 8.05 (t, 1 H), 8.03 (s, 2 H), 7.96 (s, 4 H), 7.94 (d, $^3J = 8.4$ Hz, 4 H), 7.71 (d, $^3J = 8.4$ Hz, 4 H), 7.50 (dd, $^4J = 1.6$ Hz, $^3J = 8.7$ Hz, 4 H), 7.44 (d, $^3J = 8.7$ Hz, 4 H), 1.48 (s, 36 H). ^{13}C NMR (100 MHz, CDCl_3 , ppm): δ 191.8, 146.9, 143.1, 142.1, 141.3, 139.2, 138.1, 135.6, 130.4, 128.7, 128.0, 127.1, 126.2, 125.4, 123.7, 123.6, 116.3, 109.2, 34.8, 32.0. MS (EI) *m/z*: 888 (M^+), 873 ($\text{M}^+ - \text{CH}_3$), 429 ($\text{M}^+ - \text{Ph-cbz} - \text{Ph-CHO}$).

3,5-Bis[3,6-bis(*tert*-butyl)carbazol-9-yl]benzaldehyde (A3). The synthesis was performed according to the synthetic procedure described for **A1** using 1-bromo-3,5-di[3,6-bis(*tert*-butyl)carbazol-9-yl]benzene (0.71 g, 1 mmol), *n*-BuLi (0.1 g, 1.5 mmol), and DMF (0.15 g, 2 mmol) in THF (10 mL). This gave, after purification by column chromatography over silica gel with a mixture of heptane/chloroform (6:4) as eluent, 0.5 g of **A3** as a yellow solid in 75% yield. mp > 300 °C. ^1H NMR (300 MHz, CDCl_3 , ppm): δ 10.18 (s, 1 H, CHO), 8.15 (d, $^4J = 1.83$ Hz, 4 H, cbz + 2 H, Ph), 8.09 (t, 1 H, Ph), 7.50 (dd, $^4J = 1.5$ Hz, $^3J = 8.7$ Hz, 4 H, cbz), 7.46 (d, $^3J = 8.7$ Hz, 4 H, cbz), 1.47 (s, 36 H, t-Bu). ^{13}C NMR (75 MHz, CDCl_3 , ppm): δ 190.6, 143.9, 140.9, 139.3, 138.6, 129.4, 125.0, 124.0, 123.9, 116.6, 108.9, 34.8, 32.0. MS (CI) *m/z*: 661 (MH^+), 606 ($\text{M}^+ - \text{t-Bu}$).

4-[3',6'-Bis[3,5-bis(3,6-bis(*tert*-butyl)carbazol-9-yl)phenyl]carbazol-9-yl]benzaldehyde (A4). A mixture of 4-[3,6-diiodocarbazol-9-yl]benzaldehyde (0.174 g, 0.33 mmol), 4-[3,5-[3,6-bis(*tert*-butyl)carbazol-9-yl]phenyl]boronic acid (0.45 g, 0.66 mmol), and an aqueous solution

(20) Demas, J. N.; Crosby, G. A. *J. Phys. Chem.* **1971**, *75*, 991–1024.

(21) Neugebauer, F. A.; Fisher, H.; Bamberger, S.; Smith, H. O. *Chem. Ber.* **1972**, *105*, 2686–2691.

of sodium carbonate (2M, 0.88 g, 0.83 mmol) in THF (10 mL) was placed in a flask and stirred. Nitrogen was bubbled through the reaction mixture for 5 min to remove dissolved air. Then, tetrakis(triphenylphosphine)palladium(0) (0.08 g, 0.066 mmol) was added, and the mixture was heated at 70 °C overnight. The reaction mixture was then poured in methanol, and the precipitate was collected by filtration and purified over silica gel with a mixture of heptane/chloroform (8:2) to give 0.75 g of **A4** as a yellow solid in 50% yield. mp > 300 °C. ¹H NMR (300 MHz, CDCl₃, ppm): δ 10.1 (s, 1 H), 8.47 (d, ⁴J = 1.1 Hz, 2 H), 8.18 (d, ³J = 8.4 Hz, 2 H), 8.13 (d, ⁴J = 1.8 Hz, 8 H), 7.99 (d, ⁴J = 1.8 Hz, 4 H), 7.85 (d, ³J = 8.4 Hz, 2 H), 7.81 (dd, ⁴J = 1.5 Hz, ³J = 8.4 Hz, 2 H), 7.75 (t, 2 H), 7.61 (d, ³J = 8.8 Hz, 2 H), 7.53 (d, ³J = 8.8 Hz, 8 H), 7.45 (dd, ⁴J = 1.8 Hz, ³J = 8.8 Hz, 8 H), 1.44 (s, 72 H). ¹³C NMR (75 MHz, CDCl₃, ppm): δ 190.8, 144.6, 143.2, 142.8, 140.6, 140.1, 139.0, 135.0, 132.8, 131.6, 126.8, 126.0, 124.6, 123.8, 123.6, 122.6, 119.4, 116.4, 110.6, 109.2, 34.7, 32.0. MS (ES) *m/z*: 1532 (MH⁺).

4-[3,6-Bis(3,6-bis(*tert*-butyl)carbazol-9-yl)carbazol-9-yl]benzaldehyde (A5). The synthesis was performed according to the synthetic procedure described for **A1** using *N*-(4-bromophenyl)-3',6'-[3,6-bis(*tert*-butyl)carbazol-9-yl]carbazole (0.2 g, 0.23 mmol), *n*-BuLi (0.023 g, 0.34 mmol), and DMF (0.034 g, 0.46 mmol) in THF (10 mL). This gave, after purification by column chromatography over silica gel with a mixture of heptane/chloroform (7:3) as eluent, 0.027 g of **A5** as a white solid in 30% yield. mp > 300 °C. ¹H NMR (300 MHz, CDCl₃, ppm): δ 10.17 (s, 1 H), 8.25 (d, ⁴J = 1.8 Hz, 2 H), 8.23 (d, ³J = 8.4 Hz, 2 H), 8.16 (d, ⁴J = 1.8 Hz, 4 H), 7.96 (d, ³J = 8.4 Hz, 2 H), 7.72 (d, ³J = 8.8 Hz, 2 H), 7.64 (dd, ⁴J = 1.8 Hz, ³J = 8.8 Hz, 2 H), 7.46 (dd, ⁴J = 1.8 Hz, ³J = 8.8 Hz, 4 H), 1.46 (s, 36 H). ¹³C NMR (75 MHz, CDCl₃, ppm): δ 190.9, 142.8, 142.7, 140.0, 139.6, 135.2, 131.7, 131.6, 127.0, 126.2, 124.6, 123.6, 123.2, 119.4, 116.3, 111.1, 109.0. MS (ES) *m/z*: 826 (MH⁺).

4-[3',6'-Bis(4-(3,6-bis(*tert*-butyl)carbazol-9-yl)phenyl)carbazol-9-yl]benzaldehyde (A6). The synthesis was performed according to the synthetic procedure described for **A4** using 4-[3,6-diiodocarbazol-9-yl]benzaldehyde 5.66 (0.52 g, 1 mmol), 4-[3,6-bis(*tert*-butyl)carbazol-9-yl]phenyl boronic acid (0.8 g, 2 mmol), an aqueous solution of sodium carbonate (2M, 0.26 g, 2.5 mmol), and tetrakis(triphenylphosphine)palladium(0) (0.07 g, 0.06 mmol) in THF (10 mL). The reaction mixture was poured in methanol, and the precipitate was collected by filtration, purified over silica gel with a mixture of heptane/chloroform (9:1), and recrystallized over methanol to give 0.6 g of **A6** as a white solid in 61% yield. mp > 300 °C. ¹H NMR (400 MHz, CDCl₃, ppm): δ 10.17 (s, 1 H), 8.55 (d, ⁴J = 1.8 Hz, 2 H), 8.22 (d, ³J = 8.4 Hz, 2 H), 8.16 (d, ⁴J = 1.5 Hz, 4 H), 7.96 (d, ³J = 8.4 Hz, 4 H), 7.92 (d, ³J = 8.4 Hz, 2 H), 7.83 (dd, ⁴J = 1.8 Hz, ³J = 8.4 Hz, 2 H), 7.69 (d, ³J = 8.4 Hz, 4 H), 7.66 (d, ³J = 8.4 Hz, 2 H), 7.50 (dd, ⁴J = 1.8 Hz, ³J = 8.4 Hz, 4 H), 7.45 (d, ³J = 8.7 Hz, 4 H). ¹³C NMR (100 MHz, CDCl₃, ppm): δ 190.9, 143.2, 142.9, 140.2, 140.1, 139.3, 137.0, 134.9, 133.8, 131.6, 128.5, 127.1, 126.8, 126.0, 124.8, 123.6, 123.4, 119.1, 116.3, 110.5, 109.3, 34.8, 32.0. MS (ES) *m/z*: 978 (MH⁺).

5,10,15,20-Tetrakis[*p*-[3,6-bis(*tert*-butyl)carbazol-9-yl]phenyl]porphyrin (P1). To a stirred mixture of aryl aldehyde **A1** (0.5 g, 1.3 mmol) and pyrrole (0.087 g, 1.3 mmol) in dichloromethane (200 mL) at room temperature was added boron trifluoride etherate (0.03 g, 0.2 mmol). After the mixture was stirred for an additional 2 h, *p*-chloranil (0.3 g, 1.2 mmol) was added and the reaction mixture was allowed to stir for 30 min at room temperature. The solvent was removed under reduced pressure, and the residue was chromatographed over silica gel using dichloromethane as eluent. The obtained product was redissolved in dichloromethane and precipitated with methanol, yielding 0.17 g of **P1** as purple solid in 30% yield. mp > 300 °C. ¹H NMR (300 MHz, CDCl₃, ppm): δ 9.13 (s, 8 H, pyrrole), 8.51 (d, ³J = 8.4 Hz, 8 H, Ph), 8.27 (d, ⁴J = 1.5 Hz, 8 H, cbz), 8.04 (d, ³J = 8.4 Hz, 8 H, Ph), 7.82 (d, ³J = 8.4 Hz, 8 H, cbz), 7.64 (dd, ⁴J = 1.8 Hz, ³J = 8.7 Hz, 8 H, cbz), 1.55 (s, 72 H, *t*-Bu), -2.56 (br s, 2 H, NH). ¹³C NMR (75 MHz,

CDCl₃, ppm): δ 143.7, 140.9, 139.7, 138.5, 136.4, 125.1, 124.3, 124.2, 120.1, 116.9, 109.9, 35.2, 32.5.

5,10,15,20-Tetrakis[3,5-bis(4-(3,6-bis(*tert*-butyl)carbazol-9-yl)phenyl)terphenyl]porphyrin (P2). The synthesis was performed according to the synthetic procedure described for **P1** using 3,5-bis-[3,6-bis(*tert*-butyl)carbazol-9-yl]phenyl]biphenyl-4-carbaldehyde **A2** (0.5 g, 0.56 mmol), pyrrole (0.038 g, 0.56 mmol), BF₃·Et₂O (0.02 g, 0.15 mmol), *p*-chloranil (0.25 g, 1.0 mmol), and dichloromethane (200 mL). This afforded, after purification by column chromatography over silica gel using a mixture of heptane/dichloromethane (7:3) as eluent, 0.13 g of **P2** as a purple solid in 25% yield. mp > 300 °C. ¹H NMR (400 MHz, CDCl₃, ppm): δ 9.07 (s, 8 H, pyrrole), 8.45 (d, ³J = 8.1 Hz, 8 H, Ph), 8.29 (d, ⁴J = 1.08 Hz, 8 H, Ph), 8.17 (s, 16 H, cbz), 8.12 (t, 4 H, Ph), 8.09 (d, ³J = 8.4 Hz, 16 H, Ph), 7.76 (d, ³J = 8.4 Hz, 16 H, Ph), 7.51 (dd, ⁴J = 1.4 Hz, ³J = 8.6 Hz, 16 H, cbz), 7.48 (d, ³J = 8.6 Hz, 16 H, cbz), 1.48 (s, 72 H, *t*-Bu), -2.56 (br s, 2 H, NH). ¹³C NMR (100 MHz, CDCl₃, ppm): δ 143.0, 142.3, 142.0, 141.7, 140.3, 139.6, 139.3, 138.0, 135.3, 128.8, 127.1, 125.8, 125.6, 125.4, 123.7, 123.6, 116.3, 109.3, 34.8, 32.0.

5,10,15,20-Tetrakis[3,5-di[3,6-bis(*tert*-butyl)carbazol-9-yl]phenyl]porphyrin (P3). The synthesis was performed according to the synthetic procedure described for **P1** using 3,5-di[3,6-bis(*tert*-butyl)carbazol-9-yl]benzaldehyde **A3** (0.5 g, 0.76 mmol), pyrrole (0.051 g, 0.76 mmol), BF₃·Et₂O (0.02 g, 0.16 mmol), *p*-chloranil (0.25 g, 1.0 mmol), and dichloromethane (200 mL). This afforded, after purification by column chromatography over silica gel using a mixture heptane/chloroform (9:1) as eluent, 0.08 g of **P3** as a purple solid in 15% yield. mp > 300 °C. ¹H NMR (300 MHz, CDCl₃, ppm): δ 9.12 (s, 8 H, pyrrole), 8.54 (d, ⁴J = 1.5 Hz, 8 H, Ph), 8.32 (t, 4 H, Ph), 8.13 (d, ⁴J = 1.8 Hz, 16 H, cbz), 7.81 (d, ³J = 8.7 Hz, 16 H, cbz), 7.50 (dd, ⁴J = 1.8 Hz, ³J = 8.7 Hz, 16 H, cbz), 1.40 (s, 72 H, *t*-Bu), -2.71 (br s, 2 H, NH). ¹³C NMR (75 MHz, CDCl₃, ppm): δ 143.4, 141.9, 140.7, 139.5, 136.4, 125.1, 124.3, 124.2, 120.1, 116.6, 109.0, 34.6, 32.0.

5,10,15,20-Tetrakis[4-[3',6'-bis(3,5-bis(3,6-bis(*tert*-butyl)carbazol-9-yl)phenyl)carbazol-9-yl]phenyl]porphyrin (P4). The synthesis was performed according to the synthetic procedure described for **P1** using 4-[3',6'-Bis[3,5-bis(3,6-bis(*tert*-butyl)carbazol-9-yl)phenyl]carbazol-9-yl]benzaldehyde **A4** (0.5 g, 0.33 mmol), pyrrole (0.02 g, 0.33 mmol), BF₃·Et₂O (0.02 g, 0.15 mmol), *p*-chloranil (0.25 g, 1.0 mmol), and dichloromethane (200 mL). This afforded, after purification by column chromatography over silica gel using a mixture heptane/chloroform (5:4) as eluent, 0.04 g of **P4** as a purple solid in 8% yield. mp > 300 °C. ¹H NMR (400 MHz, CDCl₃, ppm): δ 9.15 (s, 8 H, pyrrole), 8.60 (s, 8 H, cbz), 8.59 (d, ³J = 8.0 Hz, 8 H, Ph), 8.13 (d, ⁴J = 1.6 Hz, 32 H, cbz), 8.12 (d, ³J = 8.0 Hz, 8 H, Ph), 8.06 (d, ⁴J = 1.7 Hz, 16 H, Ph), 8.0 (d, ³J = 8.6 Hz, 8 H, cbz), 7.96 (dd, ⁴J = 1.8 Hz, ³J = 8.6 Hz, 8 H, cbz), 7.77 (t, 8 H, Ph), 7.56 (d, ³J = 8.6 Hz, 32 H, cbz), 7.46 (dd, ⁴J = 1.8 Hz, ³J = 8.6 Hz, 32 H, cbz), 143 (s, 288 H, *t*-Bu), -2.55 (br s, 2 H, NH). ¹³C NMR (100 MHz, CDCl₃, ppm): δ 143.2, 141.3, 140.2, 139.06, 132.5, 126.0, 124.5, 123.8, 123.7, 119.5, 116.4, 109.3, 34.7, 32.0.

5,10,15,20-Tetrakis[4-[3',6'-di[(3,6-bis(*tert*-butyl)carbazol-9-yl)]carbazol-9-yl]phenyl]porphyrin (P5). The synthesis was performed according to the synthetic procedure described for **P1** using 4-[3,6-bis(3,6-bis(*tert*-butyl)carbazol-9-yl)carbazol-9-yl]benzaldehyde **A5** (0.5 g, 0.6 mmol), pyrrole (0.04 g, 0.6 mmol), BF₃·Et₂O (0.02 g, 0.15 mmol), *p*-chloranil (0.3 g, 1.2 mmol), and dichloromethane (200 mL). This afforded, after purification by column chromatography over silica gel using dichloromethane as eluent, 0.1 g of **P5** as a purple solid in 20% yield. mp > 300 °C. ¹H NMR (400 MHz, CDCl₃, ppm): δ 9.23 (s, 8 H, pyrrole), 8.68 (d, ³J = 8.2 Hz, 8 H, Ph), 8.37 (d, ⁴J = 1.5 Hz, 8 H, cbz), 8.24 (d, ³J = 8.2 Hz, 8 H, Ph), 8.18 (d, ⁴J = 1.2 Hz, 16 H, cbz), 8.08 (d, ³J = 8.6 Hz, 8 H, cbz), 7.79 (dd, ⁴J = 1.6 Hz, ³J = 8.6 Hz, 8 H, cbz), 7.49 (dd, ⁴J = 1.6 Hz, ³J = 8.7 Hz, 16 H, cbz), 7.42 (d, ³J = 8.6 Hz, 16 H, cbz), 1.48 (s, 144 H, *t*-Bu), -2.45 (br s, 2 H, NH). ¹³C NMR (100 MHz, CDCl₃, ppm): δ 142.7, 141.8, 140.5, 140.3, 137.4,

136.3, 131.5, 126.3, 125.4, 124.5, 123.6, 123.3, 119.6, 116.3, 111.4, 109.2, 34.8, 32.1.

5,10,15,20-Tetrakis[4-[3',6'-bis[4-(3,6-bis(*tert*-butyl)carbazol-9-yl)-phenyl]carbazol-9-yl]phenyl]porphyrin (P6). The synthesis was performed according to the synthetic procedure described for **P1** using 4-[3',6'-bis[4-(3,6-bis(*tert*-butyl)carbazol-9-yl)phenyl]carbazol-9-yl]-benzaldehyde **A6** (0.49 g, 0.5 mmol), pyrrole (0.034 g, 0.5 mmol), BF₃·Et₂O (0.02 g, 0.15 mmol), *p*-chloranil (0.25 g, 1.0 mmol), and dichloromethane (200 mL). This afforded, after purification by column chromatography over silica gel using a dichloromethane as eluent, 0.1 g of **P6** as a purple solid in 20% yield. mp > 300 °C. ¹H NMR (400 MHz, CDCl₃, ppm): δ 9.25 (s, 1 H, pyrrole), 8.69 (s, 8 H, cbz), 8.66 (d, ³J = 7.9 Hz, 8 H, Ph), 8.20 (d, ³J = 8.2 Hz, 8 H, Ph), 8.18 (s, 16 H, cbz), 8.5 (d, ³J = 8.1 Hz, 16 H, Ph + 8 H, cbz), 8.0 (dd, ⁴J = 1.8 Hz, ³J = 8.9 Hz, 8 H, cbz), 7.73 (d, ³J = 8.2 Hz, 16 H, Ph), 7.51 (dd, ⁴J = 1.4 Hz, ³J = 8.7 Hz, 16 H, cbz), 7.48 (d, ³J = 8.7 Hz, 16 H, cbz), 1.49 (s, 144 H, cbz), -2.50 (br s, 2 H, NH). ¹³C NMR (100 MHz,

CDCl₃, ppm): δ 142.9, 141.1, 140.5, 139.4, 137.1, 136.2, 133.4, 131.7, 128.6, 127.2, 126.0, 125.2, 124.7, 123.6, 123.5, 119.3, 116.3, 110.7, 109.3, 34.8, 32.0.

Acknowledgment. We thank the University of Leuven (postdoctoral fellowship to A.H.), the Ministerie Voor Wetenschapsbeleid (Project IAP-V-3), MIUR (PRIN and FIRB-RBNE019H9K projects), and the University of Messina (PRA projects) for financial support.

Supporting Information Available: Absorption spectra of **A1** in various solvents and plot of the emission maximum of **A1** as a function of the Lippert solvent polarity. This information is available free of charge via the Internet at <http://pubs.acs.org>.

JA0514444